Proceedings of the 8th World Congress on Mechanical, Chemical, and Material Engineering (MCM'22)
Prague, Czech Republic – July 31, 2022 - August 02, 2022
Paper No. HTFF 158
DOI: 10.11159/htff22.158

Comparison of Air-Cooling on Metal Heat Sinks Using Numerical Modelling

Wannarat Rakpakdee[1], Teerapat Thungthong[1], Weerachai Chaiworapuek[1], Kanet Katchasuwanmanee[1], Sangkla Kreuawan[2], Vu Tran Tuan[3]

[1]Department of Mechanical Engineering, Faculty of Engineering, Kasetsart University
50 Ngamwongwan Road, Ladyao, Chatuchak, Bangkok 10900, Thailand
wannarat.rakp@ku.th; teerapat.thung@ku.th; fengwcc@ku.ac.th; kanet.k@ku.ac.th

[2]Real BPM Co., Ltd.
70/21ngor, Jessadavitee Road, Mahachai, Muang, Samutsakorn 74000, Thailand
sk@realbpm.co.th

[3]Hanoi University of Science and Technology
1 Dai Co Viet Road, Ha Noi, Viet Nam
vu.trantuan@hust.edu.vn

Abstract - In this paper, air-cooling models are investigated numerically on a new design of metal fin heat sinks based on the motor of the motorcycle using the Computational Fluid Dynamics (CFD) package ANSYS Fluent. The standard k - ε turbulence model was used in the numerical simulation. The domain was a rectangular geometry, and the metal fins created in the numerical model had three types: square pin, circle short pin, and circle long pin. These metal fin models were heated by a heat source at a power of 150-200 W based on the working range of the motorcycle's motor. Also, the air velocity for cooling was in the range of 40-60 km/h based on the motorcycle's speed. The temperature contours of the three models were used to compare the heat dissipation. The results showed that the thermal resistance did not change significantly when the heat source was changed. Notably, the circle long pin had the best effectiveness in dissipating heat compared to the others. The results from this research were important information that will help design and develop the heat sinks of the motor in the future.

***Keywords*:** Air-cooling, Heat sink, Numerical simulation, Thermal resistance

1. Introduction

Enhancement of heat transfer is one of the most popular issues in the engineering field. The use of fins is the passive method for increasing heat transfer by extending the surface area [1]. A heat sink is a metal device that absorbs and disperses heat away from a high-temperature object, such as those used in microelectronic devices and high-power electrical components. Heat sinks typically have built-in fans to keep the electrical components at a comfortable temperature. In other words, the heat sink module uses forced convection cooling to transfer heat from the heat source into the ambient air. Most heat sinks contain fins, which are thin metal slices attached to the heat sink's base that assists in diffusing heat over a large surface [2]. Recently, different heat sink designs have been utilized to study heat transfer enhancement because the flow characteristics of the heat sink channel change.

The effect of various perforated fin designs on heat sink effectiveness was investigated by Raza and Paul [3]. In comparison to other perforation shapes and non-perforated heat sinks, the heat sink with circular perforation has the highest heat transfer capability. Also, Fathi et al. [4] investigated five different geometries of heat sinks by finite volume simulation. The results revealed that the wavy form had the best heat transfer performance among the heat sink geometries studied. This shape showed an 11% increase in heat transfer rate when compared to a traditional plate heat sink. Haghighi et al. [5] carried out an experiment on natural convection for pin-fins with a cubic shape, fin spacing ranging from 5 to 12 mm, and fin numbers ranging from 5 to 9. When compared to plate heat sinks, they found that the cubic design has reduced thermal resistance and a higher heat transfer rate. In addition, the numerical investigations of a novel fin configuration for an air-cooled branched-wavy minichannel heat sink (BWMCHS) using air as the working fluid were studied by Kumar et al. [6]. The simulation used in the numerical analysis was the RNG k - ε model with enhanced wall treatment. The results showed

that a straight minichannel heat sink (SMCHS) performed lower than the BWMCHSs in terms of thermal performance. Besides, four unique fins with holes and slots in rectangular and circular shapes using the conjugate heat transfer model were investigated experimentally and numerically by Tariq et al. [7]. The results showed that the heat transfer coefficient of new plate-fin heat sinks is higher than that of plane fins without slots and holes. The novel plate-fin heat sinks showed a lower pressure drop than plane plate-fin heat sinks.

A new design of metal fin heat sinks was investigated in this study to improve the heat transfer of a motorcycle motor. The ANSYS Fluent Computational Fluid Dynamics (CFD) package was used to conduct the numerical simulation on three different heat sink models: square pin, circle short pin, and circle long pin. Based on the motorcycle's speed, the flow domain was a rectangular geometry with an air velocity for cooling in the range of 40-60 km/h. Also, the power provided to the heat sink was varied between 150 and 200 W to form the temperature contour and thermal resistance. These results can be used to assist in designing and improving future motorcycle motors.

2. Numerical model

In this study, the Navier-Stokes equation was solved under the Reynolds-averaged approach using the ANSYS Fluent software to predict air-cooling characteristics on metal fins. The SIMPLE algorithm was used to determine the pressure, momentum, turbulent kinetic energy, turbulent dissipation rate, specific dissipation rate, and energy. All spatial discretization values were set as second order upwind, except gradients were defined as least squares cell based to increase computational accuracy. In this study, the standard k - ε turbulence model was chosen and used to calculate the numerical results. The near-wall treatment of the k - ε turbulence model utilized enhanced wall treatment functions. Variables of under-relaxation parameters in solution control are listed in Table 1. The fluid physical properties and the turbulence model constants were set by default in the program. The program's calculations were controlled to achieve all residuals below 10^{-5} in all case studies.

Table 1: Under - relaxation factors.

Variables	Relaxation factors	Variables	Relaxation factors
Pressure	0.2	Turbulent kinetic energy	0.6
Density	1.0	Turbulent dissipation rate	0.6
Body forces	1.0	Turbulent viscosity	1.0
Momentum	0.3	Energy	0.8

The simulation of the air-cooling flow on metal fins provided a 3D rectangular flow domain with width, length, and height of 40, 160, and 40 cm, respectively, as shown in Fig. 1(a). As shown in Fig. 1(b), a symmetry boundary condition was required to reduce the element numbers for the reduction of the computing resources and time. The upper, side, and lower boundary conditions were set as the velocity inlet of each case. The flow direction was the same as the velocity at the inlet to reduce the formation of a velocity layer that would interfere with the heat transfer of the metal fin. The airflow through the metal fins varied between 40, 50, and 60 km/h, with a temperature of 28 °C at the inlet. The pressure of the air at the outlet was defined as 0 Pa, referring the atmospheric pressure.

The boundary conditions of the metal fin used in the numerical modelling are shown in Fig. 2. The metal fin had a base diameter of 16 cm and a thickness of 5 mm. The bottom surface area was conditioned to be an adiabatic wall to transfer heat over the entire area of the metal fin. In this study, the heat source area at the bottom surface was varied at 150, 175, and 200 W, corresponding to a heat flux of 27,671, 32,283, and 36,895 W/m^2, respectively.

Three models of metal fin heat sinks are shown in Fig. 3. Each metal fin's base plate was the same size but varied shapes as square pin, circle short pin, and circle long pin. The square pin had a width of 10 mm, a length of 10 mm, and a height of 10 mm. The diameter of both the circle short pin and the circle long pin was 3 mm, while the heights were 10 mm for the circle short pin and 20 mm for the circle long pin.

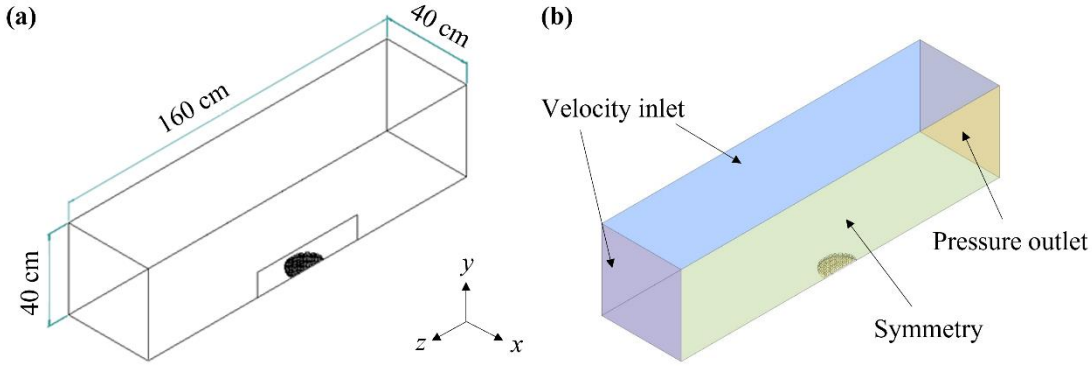

Fig. 1: (a) Physical model and (b) boundary conditions of the domain.

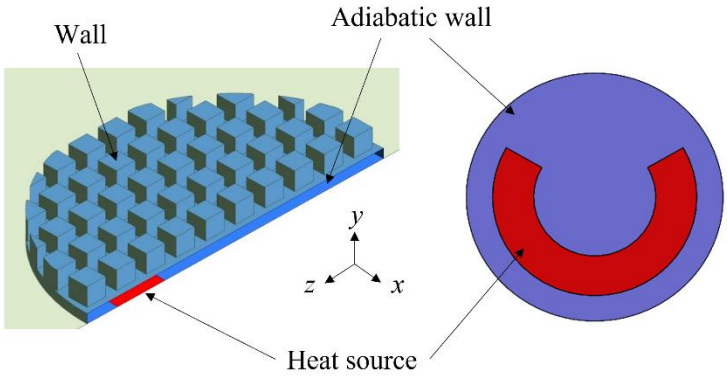

Fig. 2: Boundary conditions of metal fin.

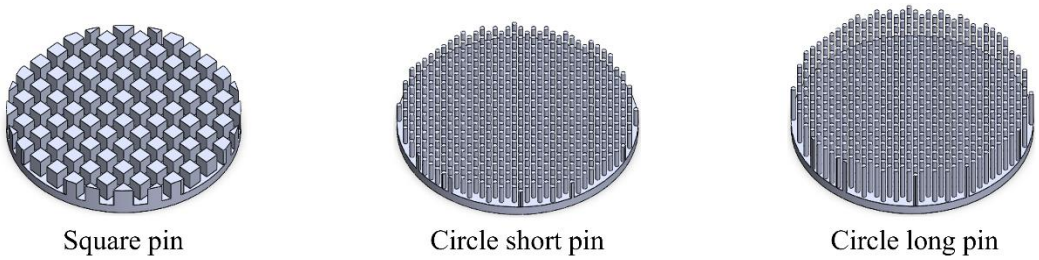

Fig. 3: Three models of metal fin heat sinks.

The process of mesh sensitivity was analysed using the average surface temperature. The numerical models of this study were to create a variable height data mesh with a 1.2-fold growth rate across all layers. It also created a high-resolution data mesh around the metal fin edge symmetry conditions to control the y^+ value of approximately 1 throughout the analysis. The domain was created with a tetrahedral mesh, with a size range of 1.2 mm to 2.8 mm and a 0.2 mm interval. Fig. 4(a) depicts the relationship between average surface temperature and the element number of the square pin model. In the figure, the estimated findings began to converge at the element number of 1,564,596 with an element size of 1.6 mm. As a result of mesh generation, the heat sink models of the square pin, circle short pin, and circle long pin had 1,564,596, 3,912,288, and 6,582,656 elements with mean mesh quality measured for skewness values of 0.236, 0.21, and 0.213, respectively. Fig. 4(b) shows the computational grid for the geometric pattern of the square pin model.

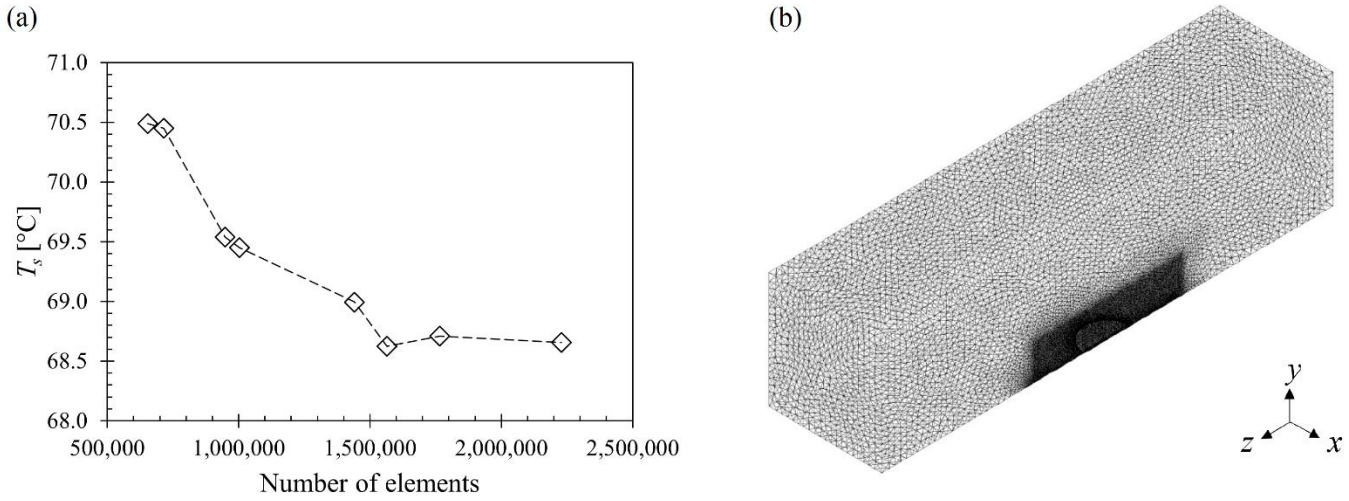

Fig. 4: (a) Mesh convergence and (b) mesh generation of modelling.

3. Data reduction

The standard k - ε turbulence model is used to solve the three-dimensional Navier-Stokes governing equations. Hence, the continuity and the Navier-Stokes equations can be expressed as following:

$$\partial\rho/\partial t = -\nabla \cdot (\rho v) \tag{1}$$

$$\rho(\partial v/\partial t + v \cdot \nabla v) = -\nabla p + \mu\nabla^2 v \tag{2}$$

where ρ is the fluid density [kg/m^3], t is the time [s], v is the velocity vector [m/s], p is the pressure [Pa], and μ is the absolute viscosity [Pa.s].

The numerical simulation of the airflow was modelled in the rectangular duct. Thus, the Reynolds number based on the hydraulic diameter of the rectangular duct can be determined as:

$$Re = \frac{\rho_a v_a D_h}{\mu_a} \tag{3}$$

where a subscript means the air. The hydraulic diameter can be calculated as:

$$D_h = \frac{4A_c}{P} \tag{4}$$

where A_c is the cross section of the duct [m^2] and P is the perimeter [m]. Normally, heat sinks are chosen primarily based on the required thermal resistance. The thermal resistance, R_{th} [°C/W], can be determined as:

$$R_{th} = \frac{(T_s - T_\alpha)}{Q_h} \tag{5}$$

where T_s is the average surface temperature of the fins [°C], T_α is the ambient temperature [°C], and Q_h is the power of the heat source [W].

4. Results and discussion

In this study, numerical simulation of the air flow through three metal fin heat sink models including the square pin, the the circle short pin, and the circle long pin was performed as the setup previously explained. The models were investigated investigated by varying the heating power of 150, 175, and 200 W and the Reynolds numbers of 373,760, 465,950, and 559,140.

The temperature distribution on the metal fins at *Re* of 373,760 and Q_h of 150 W for the square pin, circle short pin, and circle long pin is shown in Fig. 5(a)-(c). In these figures, the heat transfer across the surface area of the fins was exchanged by the airflow at a temperature of 28 °C. Because of the heat source position, the temperature distribution of the metal fins in the upstream area was found to be higher than in the downstream area. In comparison to the other models, it clearly showed that the surface temperature of the circle short pin was the highest, while the surface temperature of the circle long pin was the lowest. As a result, the circle long pin had the highest heat transfer and transferred better heat than the other models. When the heat source provided to the heat sinks increased to Q_h = 200 W, the surface temperature of the circle long pin at *Re* of 373,760 increased, as depicted in Fig. 5(d). In addition, the surface temperature of the circle long pin decreased as the *Re* increased to 465,950 and 559,140, as illustrated in Fig. 5(e) and (f), respectively. From these results, it could be concluded that the shape and height of fins are important parameters to boost the heat dissipation of the heat sinks.

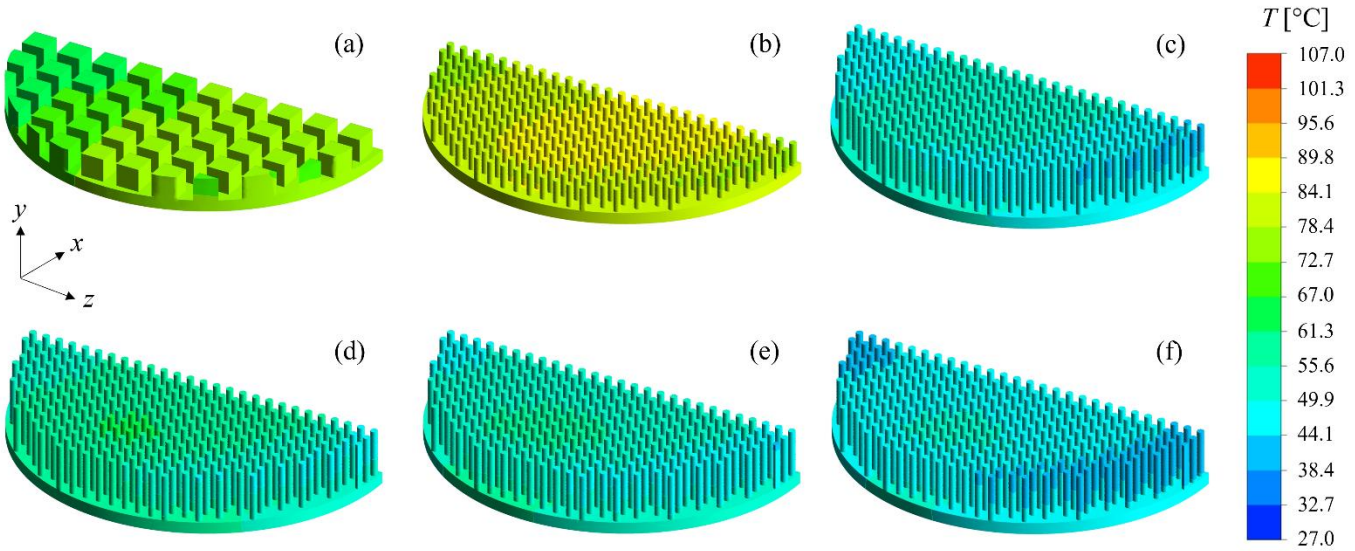

Fig. 5: Temperature contours of (a) square pin, (b) circle short pin, and (c) circle long pin at *Re* = 373,760 and Q_h = 150 W, as well as temperature contours of circle long pin at Q_h = 200 W and *Re* of (d) 373,760, (e) 465,950, and (f) 559,140.

After obtaining the temperature contours, the averaged surface temperature can be calculated and plotted against the Q_h between 150 and 200 W, as shown in Fig. 6. From the results, the average surface temperature rose as Q_h increased but decreased as *Re* increased. When the Q_h was 200 W and the *Re* was 373,760, the average surface temperature of the circle short pin was found to be the highest at 101.6 °C, while when the heat sink model was changed to the circle long pin, the averaged surface temperature dropped to 57.4 °C. It indicated that when the height of the pin was increased from 10 mm to 20 mm, the average surface temperature of the heat sinks was reduced by roughly 44%. Thus, the circle long pin produced the lowest average surface temperature in this study. Moreover, the average surface temperature of a circle short pin at *Re* of 559,140 was found to be lower than that of a square pin at *Re* of 373,760. However, the average surface temperature of all square pin cases was higher than the average surface temperature of all circle long pin cases. As a result, the circle long pin heat sink model was discovered to have the best heat exchange capability comparing with the other two types.

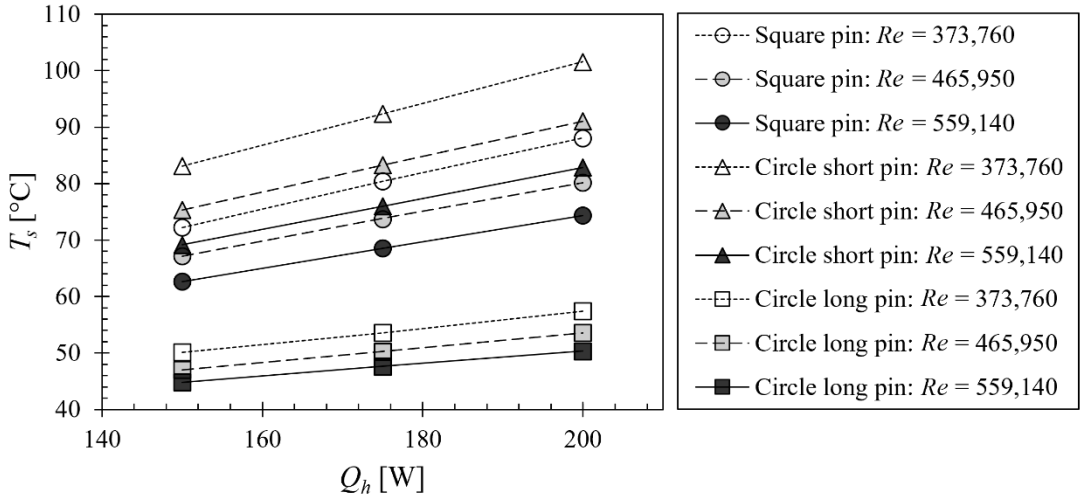

Fig. 6: Average surface temperature for three heat sink models.

Furthermore, the thermal resistance of the heat sinks can be calculated via Eq. (5) and plotted against the Q_h between 150 and 200 W, as shown in Fig. 7. In the figure, the thermal resistance of all three models decreased as *Re* increased. Nevertheless, the thermal resistance had no substantial change by changing the Q_h. The circle short pin case at the *Re* of 373,760 had the highest thermal resistance of 0.368, while the circle long pin case at the *Re* of 559,140 had the lowest thermal resistance of 0.112 °C/W. Meanwhile, the thermal resistance of the square pin model was found to be in the range of 0.231-0.300 °C/W during the *Re* of 373,760-559,140. As a result, the heat sink model with the circle long pin was the most effective at dissipating heat when compared to the other models.

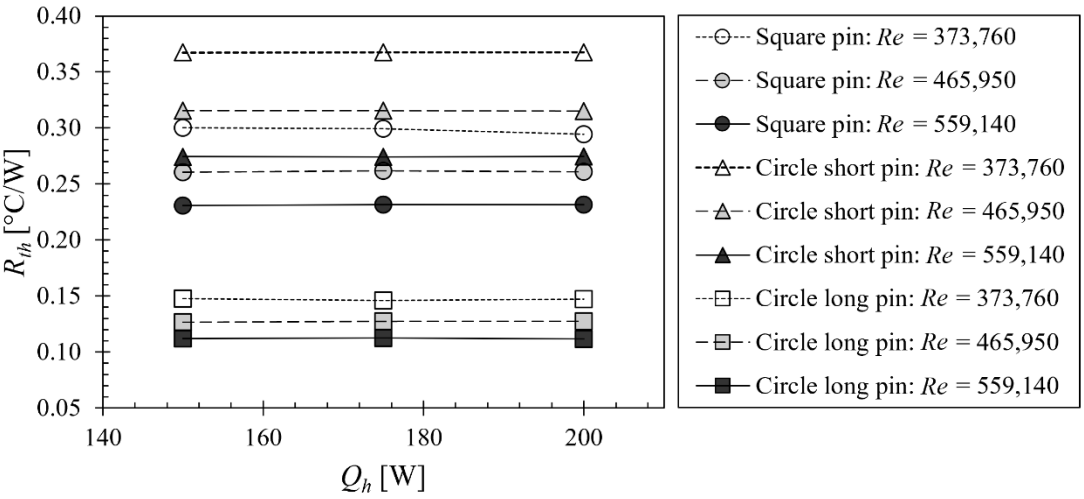

Fig. 7: Thermal resistance for three heat sink models.

5. Conclusion

In this analysis, three models of metal fin heat sinks are investigated numerically using the commercial CFD package ANSYS Fluent. The three models in this study were the square pin, the circle short pin, and the circle long pin. In the simulation, the air-cooling flow on metal fins was assigned to be a 3D rectangular airflow boundary with a symmetrical numerical model that was calculated by the standard k - ε turbulence model. The airflow through the metal fins was varied at 40, 50, and 60 km/h, corresponding to *Re* of 373,760, 465,950, and 559,140, respectively. Also, the

heat source area at the bottom surface of the heat sinks was adjusted to 150, 175, and 200 W, corresponding to a heat flux of 27,671, 32,283, and 36,895 W/m^2. The current investigation yielded the following results:

1. For all heat sinks, the average surface temperature increased as Q_h increased but decreased as *Re* increased.
2. The circle short pin had the highest average surface temperature, whereas the circle long pin had the lowest.
3. When the Q_h was changed, the thermal resistance did not change substantially.
4. In this study, the circle long pin had the best ability to dissipate heat.

Acknowledgements

The authors express their sincere thanks to the Faculty of Engineering, Kasetsart University, Bangkok, Thailand for financial support.

References

[1] D. S. Khudhur, R. C. Al-Zuhairy and M. S. Kassim, "Thermal analysis of heat transfer with different fin geometry through straight plate-fin heat sinks," Int. J. Therm. Sci., vol. 174, pp. 107443, 2022.

[2] H. T. Dhaiban and M. A. Hussein, "The Optimal Design of Heat Sinks: A Review," J. Appl. Comput. Mech., vol. 6, no. 4, pp. 1030-1043, 2020.

[3] F. Raza and A. Paul, "Evaluating the performance of heat sink having different shapes of perforated fins," Int. J. Res. Trends Innov., vol. 4, no. 9, pp. 2456-3315, 2019.

[4] S. Fathi, M. E. Yazdi and A. Adamian, "Numerical investigation of heat transfer enhancement in heat sinks using multiple rows vortex generators," J. Theor. Appl. Mech., vol. 58, no. 1, pp. 97-108, 2020.

[5] S. S. Haghighi, H. R. Goshayeshi and M. R. Safaei, "Natural convection heat transfer enhancement in new designs of plate-fin based heat sinks," Int. J. Heat Mass. Tran., vol. 125, pp. 640-647, 2018.

[6] R. Kumar, B. Tiwary and P. K. Singh, "Influence of secondary pass location on thermo-fluidic characteristic on the novel air-cooled branched wavy minichannel heat sink: A comprehensive numerical and experimental analysis," Appl. Therm. Eng. vol. 182, pp. 115994, 2021.

[7] A. Tariq, K. Altaf, S. W. Ahmad, G. Hussain and T. A. H. Ratlamwala, "Comparative numerical and experimental analysis of thermal and hydraulic performance of improved plate fin heat sinks," Appl. Therm. Eng. vol. 182, pp. 115949, 2021.